PHYSICAL REVIEW B VOLUME 3, NUMBER 8 15 APRIL 1971

F Centers in Ionic Crystals: Semicontinuum-Polaron Models and Polarizable-Ion Models

Herbert S. Bennett
National Bureau of Standards, Washington, D. C. 20234
(Received 31 August 1970)

The three lowest-lying *F*-center states for KCl, CaO, and CaF_2 are calculated within the framework of five semicontinuum-polaron models and one polarizable-ion model. The movement of the nearest-neighbor ions to the *F* center and the *F* electron are treated in a self-consistent manner in these models. Exact solutions to these models for the states involved in the transitions of optical absorption and emission are obtained numerically. In addition, the internal Stark effect due to noncubic phonons is estimated. The absorption energy, the emission energy, and the lifetime of the first excited state are evaluated for the six models. It is shown that a semicontinuum-polaron model agrees best with the experimental results for KCl and that the polarizable-ion model gives the best results for CaO and CaF_2. In addition, the semicontinuum-polaron model and the internal Stark effect predict that the relaxed excited state in KCl consists of a strong mixing of $2p$-like and $2s$-like states which are spatially diffuse.

I. INTRODUCTION

The *F* center in ionic crystals consists of one electron (the *F* electron) localized about a vacant anion site, regardless of the missing anion valence. Even though the *F* center is one of the simplest defects which may occur in ionic crystals, calculations of its energy states have been a challenge to theoreticians ever since Tibbs first undertook such calculations for the alkali halides.[1] Such calculations are even today unsatisfactory in many cases when one studies the lifetimes of relaxed excited states, the phonon structure, and the spatial extents of the *F*-electron wave functions.[2,3] A relaxed state of the *F* center $|F_\eta^*\rangle$, is one for which the *F*-electron state with a given symmetry (denoted by η) has existed for a time long enough to allow the lattice to accommodate itself to the defect. The lowest-lying relaxed excited state of the *F* center will be denoted by $|F^*\rangle$. The unrelaxed state $|F_\eta\rangle$ arises when the electronic state $|F\rangle$ has existed for such a short time that the lattice has not had sufficient time to accommodate itself to the new charge density associated with the *F* electron.

The study of *F* centers aids in understanding the photochromic process in the alkali halides.[4] A photochromic material is a medium that can be erased, addressed, and interrogated by light. The electron energy states of isolated impurities or defects which lie in the band gap of insulators play a very important role in determining how photochromic materials function. The *F*-center states treated in the present calculations are such examples. In particular, the *F* center in KCl exhibits photochromic properties. The "erase" photochromic mechanism depends in part upon the photoexcitation of the *F* electron to a high-lying excited state. The excited *F* electron then is ionized into the conduction band by thermal phonons. A conduction electron can be trapped by an *F* center to form an F' center. The F' center consists of two electrons localized about a vacant anion site. The "write" photochromic mechanism consists of the ionization by light of one electron in the F' center to form the *F* center again. The "read" photochromic mechanism entails the photoexcitation of the *F* center to a low-lying excited state. The lifetimes of the low-lying excited *F*-center states play a very important role in determining how well a potential photochromic medium performs.

Two basic models from which the electronic structure of the *F* center may be calculated exist. These are the semicontinuum (or semicontinuum-polaron) models (SP) and the Hartree (or Hartree-Fock) polarizable-ion models (PI). Both classes of models reduce a many-electron problem to an effective one-electron (the *F* electron) problem and treat the lattice polarization and the *F* electron in a self-consistent manner. They differ markedly in their treatment of the effective interaction between the *F* electron and the anion vacancy due to the ionic polarization. The vacancy may be viewed as an infinite effective-mass hole having a charge $Z_v > 0$. The SP models contain an approximate expression for the *F*-electron–vacancy interaction which is based upon the Haken theory of Wannier excitons.[5,6] This interaction thereby allows the ionic polarization to follow to some extent the motion of the *F* electron when the latter is in a large orbit. The PI models assume that the *F*-electron orbit will be small enough so that the ionic polarization cannot follow the rapid changes in the *F*-electron motion.

Some SP and PI models were discussed in previ-

ous papers[7,8] within the context of variational procedures employing hydrogenic trial wave functions for the F electrons.[9] It was found in Ref. 7 that a SP model for the F center was most successful for KCl and NaCl, was successful only for optical absorption in CaF_2, SrF_2, and BaF_2, and gave inconclusive results for MgO and CaO. It was demonstrated also in Ref. 8 that a PI model was rather successful for CaO, was successful with some qualifications for MgO, and was least successful in the alkali halides and alkaline-earth fluorides. Success for the above models was determined by the extent to which they agree with experimental data. Judgments about the success of a given model for the F center in the alkaline-earth fluorides are apt to be inconclusive because the only known experimental data treat the absorption of the F center and this is probably least sensitive to the physical details of a model.

All theoretical treatments of the F center consider models with mathematical descriptions which are by necessity much simpler than those of the real F center. The above treatments of the F center use trial or variational wave functions. Thus, they are approximate solutions to a model problem. Consequently, two questions arise in such treatments. Namely, how well do the approximate solutions give the exact properties of the model and how well does the model represent the properties of the real system? Solving the model exactly answers best the first question. Comparing the predictions made by such solutions to the model with the experimental properties answers the second question.

In this paper, the necessity for asking the first question is removed. The procedure is to solve numerically the Hartree-Fock-Slater (HFS) equations for the F center given by the SP and PI models which were studied in Refs. 7 and 8. Because variational wave functions are not employed, the first question does not arise. The second question does remain. Namely, how well does the model represent the real system? The numerically computed solutions give the exact properties of the model. If one has confidence that the assumptions contained in the model are physically reasonable, then comparing the predictions made by the model with the experimental data answers the second question.

The models for the present calculations include in a classical treatment the ionic polarization of the nearest-neighbor ions. The symmetry properties of the F-electron wave function for the initial and final states of an optical transition are specified first. The computer finds the minimum value of the total energy for the F center in its initial state as a function of the distance $r_1\sigma$ by which the nearest-neighbor ions move radially from their sites in a perfect lattice (ionic polarization). The nearest-neighbor distance in the perfect lattice is r_1. The computer then determines the total energy for the F center in its final state of the optical transition from the same nearest-neighbor ionic polarization as that for the initial state. This is in accordance with the Franck-Condon principle for ions which behave classically. The distant ions for SP models may violate to some extent the Franck-Condon principle.

The three lowest-lying F-center states for some alkali halides, alkaline-earth oxides, and alkaline-earth fluorides are studied here within the framework of selected SP and PI models. These models predict either one of the following orders for the F-center energy levels: $|1s;\sigma\rangle$, $|2p;\sigma\rangle$, and $|2s;\sigma\rangle$, or $|1s;\sigma\rangle$, $|2s;\sigma\rangle$, and $|2p;\sigma\rangle$. The total F-center state is designated by the notation $|\eta;\sigma\rangle$. The symbol η represents the generic quantum numbers of the F-center state and the symbol σ characterizes the crystal potential which the F electron in state η experiences. For example, the F-center state $|2p;\sigma\rangle$ has an F-electron part which transforms as a $2p$-like electronic wave function transforms under the cubic point group. The $|2s;\sigma\rangle$ and $|2p;\sigma\rangle$ states both lie above the $|1s;\sigma\rangle$ state, but whether the $|2s;\sigma\rangle$ state lies above or below the $|2p;\sigma\rangle$ state depends both upon the ionic polarization of the crystal potential σ and the model from which these states are computed. The relative ordering and spacing of the energies for the $|2s;\sigma\rangle$ and $|2p;\sigma\rangle$ states and the spatial extents of these states appreciably influence the predicted lifetime of the relaxed excited state of the F center, $|F^*\rangle$.

The present calculations do not account for the Jahn-Teller effect on the $2p$-like states. Because the $|2p;\sigma\rangle$ state is threefold degenerate for the SP and PI models, the ions neighboring the F center should move from their perfect lattice sites in such a manner that the $2p$-like F electron experiences a potential having a symmetry which is lower than the cubic symmetry of the perfect lattice. That is, the $2p$ state should be unstable against lower symmetry distortions of the nn ions.

Swank and Brown[10] were the first to measure the radiative lifetime of the relaxed excited state $|F^*\rangle$. The radiative lifetime of the state $|F^*\rangle$ in KCl and NaCl is about two orders of magnitude greater than the values which are expected from the respective experimental oscillator strengths in absorption. Experimental data on the radiative lifetimes of $|F^*\rangle$ in[11,12] MgO and CaO suggest that they are comparable to the values expected from the respective oscillator strengths in absorption. Experimental data on the emission properties of the F center in CaF_2, SrF_2, and BaF_2 have not been reported in the literature.

It is shown in this paper that the agreement between the experimental values for the lifetimes of the state $|F^*\rangle$ in KCl and NaCl and the theoretical

values given in Refs. 7 and 13 is fortuitous. The HFS equations for the SP(HF) model of Ref. 7 are solved here exactly by numerical methods to give the $1s$-, $2p$-, and $2s$-like wave functions for the F electron. It is found that because the spatial extents of the respective initial and final states entering the transition matrix elements for absorption and for emission are similar, the predicted lifetime of the $|F^*\rangle$ state in KCl is substantially smaller than the experimental lifetime. In addition, the energy of the $|2s;\sigma_1\rangle$ state is found for emission to be near the energy of the $|2p;\sigma_1\rangle$ state. The quantity σ_1 characterizes the crystal potential for emission. This last result indicates that introducing some mechanism which leads to a mixing of the $|2s;\sigma_1\rangle$ and $|2p;\sigma_1\rangle$ states may account for the long lifetime.

One possible mixing mechanism arises from the fluctuating internal electric fields of noncubic longitudinal-optical phonons moving through the F center. Because the vibrations associated with such phonons mix $2s$- and $2p$-like states, their vibronic motions near the F center transform as the Γ_{15} representation of the cubic point group transforms. They produce under the proper conditions an effective Stark effect at the F center. Thus, the noncubic phonons can lead to states which contain a mixture of $|2s;\sigma\rangle$ and $|2p;\sigma\rangle$ states. That is, not only may the spatial extent of the F-electron wave function change from absorption to emission but also, its angular character may change as well. Hence, the exact numerical solutions to the SP(HF) model and the subsequent necessity to introduce a mechansim which mixes $|2s;\sigma\rangle$ and $|2p;\sigma\rangle$ states in order to account for the long radiative lifetime of $|F^*\rangle$ suggest that the $|2s;\sigma\rangle$ state plays an important role, comparable to that of the $|2p;\sigma\rangle$ state, in the emission process of the F center in some alkali halides.

Even though the lifetime computed from the approximate solutions is much larger than that computed from the exact solutions to the SP(HF) model for KCl, it is shown that the approximate and exact absorption energies agree to within 10% of each other and to within 15% of the experimental absorption energy. The approximate and exact emission energies are equal and agree to within 3% of the experimental emission energy.

Because exact solutions to the PI(2) model of Ref. 8 require excessive amounts of computer time, a simplified version of the PI(2) model is introduced, namely, the PI(3) model. The F electron experiences in this PI(3) model only the spherically symmetric part of that point-ion potential for which the nearest-neighbor ions move, in an otherwise perfect lattice, self-consistently to accommodate themselves to the charge density associated with the F electron. It is found for CaO that the approximate PI(2) absorption energy and the exact PI(3) absorption energy agree to within 3% of each other and to within 10% of the experimental absorption energy. The exact PI(3) emission energy for CaO equals the experimental emission energy and agrees to within 2% of the approximate PI(2) emission energy. All lifetimes for CaO agree to within an order of magnitude and are comparable to the lifetime expected from the experimental oscillator strength in absorption. The absorption energies computed from the approximate solutions to the SP(HF) model for CaF_2 agree to within 17% of each other and to within 18% of the experimental absorption energy. The agreement between the PI models for CaF_2 is better. The approximate PI(2) absorption energy for CaF_2 agrees to within 10% of the exact PI(3) absorption energy and to within 10% of the experimental absorption energy. Experimental emission and lifetime data are not available for CaF_2. Because marginal differences exist between the approximate and exact solutions to the models for CaO and CaF_2, most of the discussion in the present paper is devoted to the F center in KCl. All the models for which exact solutions have been obtained are summarized, however, in Secs. III and IV.

These above results suggest that as the lifetime and the Stokes shift (the differences between the absorption and emission energies) become large, the more suspect the predictions based upon approximate solutions become and the more important the roles played by the $|2s;\sigma\rangle$ states become.

Chiarotti *et al.*[14] have reported on the importance of the $|2s;\sigma\rangle$ states for the quadratic Stark effect of the F center in KCl. They have interpreted the effect in terms of a system of two nearly degenerate excited states, $2s$-like (Γ_1) and $2p$-like (Γ_{25}), which are mixed by the electric field. They have found that the energy of the $2s$-like state lies 0.004 a.u. (0.11 eV)[15] above the energy of the $2p$-like state.

Other researchers also have reported on the importance of the $|2s;\sigma\rangle$ states for the emission process of the F center in the alkali halides. The recent experiments of Bogan and Fitchen,[16] Kuhnert,[17] and Stiles *et al.*[18] cannot be explained by the diffuse $2p$-state methods.[7,13] The authors of Refs. 16 and 17 have studied the Stark effect on the relaxed excited state $|F^*\rangle$ of the F center. They have concluded that the $|F^*\rangle$ state has a considerable amount of $|2s;\sigma\rangle$ character in it. Stiles *et al.*[18] have measured in several alkali halides, including KCl, the change in the radiative lifetime induced by an applied electric field and by increasing the temperature. These authors have reported that both the electric field and the temperature effects on the radiative lifetime are quantitatively consistent with the mixed-state model proposed by Bogan and Fitchen.[16]

Some theoretical calculations which include the $|2s;\sigma\rangle$ state have been made concurrently with the above experimental work. Fowler *et al.*,[19] Wood and Öpik,[20] and Bennett[21] all have found that the $|2s;\sigma\rangle$ and $|2p;\sigma\rangle$ states for emission in some alkali halides may have energy eigenvalues which are close together. Wood and Öpik[20] have reported that as the lattice distorts to accommodate the relaxed excited state $|F^*\rangle$ in KCl, the $|2s;\sigma\rangle$ state crosses the $|2p;\sigma\rangle$ state and finally has an energy 0.003 a.u. (0.08 eV) lower than the energy of the $|2p;\sigma\rangle$ state.

It is shown in this paper that the exact numerical solutions to both the SP models of Ref. 7 for KCl and to slight modifications of these models all predict that the $|2s;\sigma\rangle$ and $|2p;\sigma\rangle$ states have energies which lie very close to one another for the relaxed excited state $|F^*\rangle$. The $|2s;\sigma\rangle$ state lies for some models above the $|2p;\sigma\rangle$ state and it lies for other models below the $|2p;\sigma\rangle$ state. Care must be exercised whenever the $|2s;\sigma\rangle$ state and the $|2p;\sigma\rangle$ are predicted by these models to have an energy separation which is less than 0.01 a.u. The exact solutions to the above models are mathematically accurate to $\pm 0.1\%$. However, because some of the terms appearing in the Hamiltonians which describe these models are known to a physical accuracy of at best $\pm 5\%$, the relative locations of the $|2s;\sigma\rangle$ and $|2p;\sigma\rangle$ states become questionable whenever the energy difference between these two states is less than 0.01 a.u.

The present calculations are consistent with the view that the relaxed excited state $|F^*\rangle$ of the F center in KCl consists of nearly degenerate and strongly mixed $|2s;\sigma\rangle$ and $|2p;\sigma\rangle$ states. Neither Fowler *et al.*[19] nor Wood and Öpik[20] have considered the mixing of $|2s;\sigma\rangle$ and $|2p;\sigma\rangle$ states in their calculations. The calculations reported here do include the mixing of the $|2s;\sigma\rangle$ and $|2p;\sigma\rangle$ states which result from an effective internal electric field at the F center for emission. In fact, it is found that among the models examined here for KCl only one predicts a value for the radiative lifetime which agrees reasonably well with the experimental value for the lifetime. This particular model is a slight modification of the SP(HF) of Ref. 7 [SP(HF_1)], which originally was developed to reduce the amount of computer time required to solve the HFS equations for the SP(HF) model.

The classical ionic lattice and its role in accommodating the F electron are reviewed in Sec. II. Sections III and IV contain the presentations of the six models for which exact solutions have been obtained numerically. The theoretical expressions for those quantities which are measured in the optical absorption and emission experiments are given in Sec. V. In Sec. VI, the numerical results for the six models are tabulated and compared with past theoretical results and with experiments. Section VII contains a statement of the intuitive ideas associated with the internal Stark effect. The application of the internal Stark effect to the SP(HF_1) model of the F center in KCl and the improved value for the lifetime of the excited state are also presented in Sec. VII. Section VIII contains a brief summary of the main concepts developed in the present research. Finally, the notation used to denote the several models for the F center is listed in the Appendix.

II. CLASSICAL IONIC LATTICE

The models for the F center presented below contain the same treatment of the lattice energy and differ only in their treatment of the contribution to the F-center energy due to the electronic and ionic polarizations. Discussions of the total crystal Hamiltonian and the classical ionic lattice are given in Secs. II and III of Ref. 7. Because the results of Secs. II and III of Ref. 7 will be used here, the contents of those two sections are summarized below.

Using the Born-Oppenheimer approximation, the one-electron Hamiltonian for the F center is written as the sum of two terms,

$$H_T(\vec{r},\vec{R}) = H_F(\vec{r},\vec{R}) + H_L(\vec{R}) \ . \tag{1}$$

The expectation value of the operator H_F gives us the F-electron energy, while the expectation value of H_L, which contains no F-electron operators, gives us the lattice energy of the crystal.

The optical absorption and emission which the F center may undergo are studied. The F center, which is originally in its ground state $|F_0^*;\sigma_0\rangle$, becomes excited into the unrelaxed state $|F_1;\sigma_0\rangle$. The unrelaxed state $|F_1;\sigma_0\rangle$ is assumed to be a quasistationary state with an electronic wave function calculated from the same crystal potential as that for the relaxed ground state $|F_0^*;\sigma_0\rangle$. The lattice then relaxes and thereby the crystal potential which the F electron experiences changes. The excited electronic state calculated from the relaxed crystal potential $|F_1^*;\sigma_1\rangle$ may differ from the unrelaxed excited state $|F_1;\sigma_0\rangle$. The F center then may undergo a transition to the unrelaxed ground state $|F_0;\sigma_1\rangle$ with an electronic wave function calculated from the same crystal potential as that for the relaxed excited state $|F_1^*;\sigma_1\rangle$. A configuration, coordinate diagram which illustrates the F-center states discussed above, is presented in Fig. 1.

It is necessary to compute the change in the lattice energy due to replacing an anion with an F-center electron. A vacancy at the anion site $\vec{r}_0 = \vec{0}$ of charge Z_0 is created first by adding an effective charge $Z_v = Z_0$ at $\vec{r}_0 = \vec{0}$. The fictitious lattice state, for which no lattice relaxation is permitted after the creation of the anion vacancy,

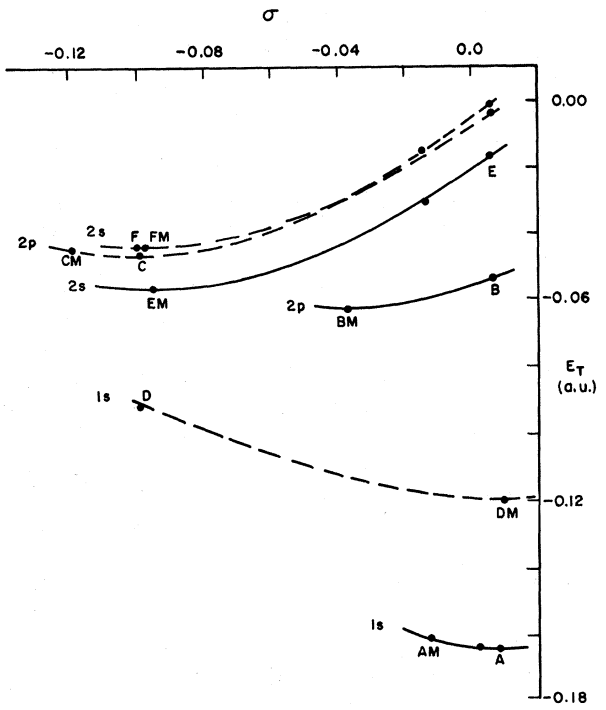

FIG. 1. Configuration coordinate diagram given by SP(HF_1) model for the F center in KCl in which the nn ions obey the Franck-Condon principle. The quantity E_T is the total energy of the F center, and σ gives the nn radial motion (ionic polarization); $r_1' = r_1(1-\sigma)$, where r_1 is the nn distance in the perfect lattice. The points A, B, E, D, C, F correspond, respectively, to the states $|1s;\sigma_0\rangle$, $|2p;\sigma_0\rangle$, $|2s;\sigma_0\rangle$, $|1s;\sigma_1\rangle$, $|2p;\sigma_1\rangle$, and $|2s;\sigma_1\rangle$. The F-electron wave function is $1s$-like for curves AM-A and D-DM; it is $2p$-like for curves BM-B and CM-C; and it is $2s$-like for curves EM-E and F-FM. The electronic polarization responds for all states to rapid changes in the F-electron wave function. The distant ionic polarization is zero for the solid curves (absorption); it is given in terms of an effective dielectric constant for the dashed curves (emission). The solid curves are coplanar and lie in a plane parallel to the $E_T - \sigma$ plane. The dashed curves are coplanar and lie in a place which is parallel to the $E_T - \sigma$ plane and which does not coincide necessarily with the plane in which the solid curves lie.

will serve as the reference energy for the lattice part of the total F-center Hamiltonian. The change in the lattice energy ΔE_L (vacancy, distortion) due to replacing an anion with an F-center electron is computed in terms of classical ionic lattice theory. The nearest-neighbor (nn) ions move radially from r_1 to $r_1' = r_1(1-\sigma)$ in order to accommodate the F-center charge density. The total F-center charge density $\rho_d(\vec{r})$ is given by the relation,

$$\rho_d(\vec{r}) = \rho_F(\vec{r};\eta) + \rho_v(\vec{r}) , \tag{2}$$

where the F-electron change density is

$$\rho_F(\vec{r};\eta) = -e\psi_\eta^*(\vec{r})\psi_\eta(\vec{r}) \tag{3}$$

and where the charge density of the vacancy is

$$\rho_v(\vec{r}) = Z_v \delta^3(\vec{r}) . \tag{4}$$

The F-electron wave function is $\psi_\eta(\vec{r}) = \langle \vec{r} \mid F_\eta;\sigma\rangle$, where the quantity F_η denotes the symmetry properties of the F electron. The wave functions are normalized to the crystal volume:

$$\int \psi_\eta^*(\vec{r})\psi_\eta(\vec{r})\, d^3r = 1 . \tag{5}$$

The effective vacancy charge is Z_v. The δ function $\delta^3(\vec{r})$ means that the effective vacancy charge Z_v is treated as a point charge. The quantity $Z_F = -e$ is defined and the magnitude of the electronic charge is e.

The change in the lattice energy is written as the sum of many terms. There are many ways to carry out the summations. The method given by Eqs. (17) and (18) of Ref. 7 is chosen, i.e., the lattice energy has the form ΔE_L (vacancy, distortion) = $\Delta E_e + \Delta E_r$, where ΔE_e is the change in electrostatic energy and ΔE_r is the change in the effective repulsive energy which takes the Pauli exclusion principle between the ith- and jth-ion cores into account. Because the van der Waals terms increase the formation energy by about 5% and decrease the distortion by about 4%, and because the F-center-electronic part of the Hamiltonian is not expected to be accurate to within 5% of the experimental results, the van der Waals terms are not included in the expression for the cohesive energy from which the lattice energy is computed. In addition, because the inward distortion compatible with a compact F center will be excessive if the next-nearest-neighbor repulsions for the oxides are neglected, both first- and second-nn repulsive terms are included in the cohesive energy. The repulsive energy contribution to the cohesive energy is expressed by means of the empirically determined Born-Mayer exponential form. Again, the reader is referred to Sec. III of Ref. 7 for the details.

III. SEMICONTINUUM-POLARON MODELS

Five semicontinuum-polaron Hamiltonians characterizing the F center will be developed in this section. Two of the five SP Hamiltonians have been studied in Ref. 7, namely, the SP(HF) and SP(QA) models, where HF and QA mean, respectively, that the optical polarization is computed according to the continuum Hartree approximation and according to the quasiadiabatic approximation. Only variational solutions have been found for these two models. The predictions computed from the exact numerical solutions to those models will be reported in Sec. V. Three modifications of the SP(HF) and SP(QA) models also will be presented here. They will be called the SP(HF_1), SP(QA_1), and SP(EI_1) models. Because many of the energy

terms are common to all of the models, a general discussion of semicontinuum-polaron models will be presented first. Then each of the five models will be given.

The vacancy is viewed in the semicontinuum approximation as a spherical cavity of radius R (the Mott-Littleton radius) in a continuous dielectric medium characterized by the static and high-frequency dielectric constants ϵ_0 and ϵ_∞, respectively. The expression,

$$W_p = Z_0^2[1-(1/\epsilon_0)]/R\ , \tag{6}$$

relates the Mott-Littleton radius to the electronic polarization energy W_p. This is the energy required to move an ion of charge Z_0 to the surface of a rigid lattice.

The one-electron Hamiltonian for the F-center electron is written in the form

$$H_F = \frac{\vec{p}^2}{2m} + \sum_{\nu\neq 0}{}' V_\nu(\vec{r}-\vec{R}_\nu) + V_p(\vec{r})\ , \tag{7}$$

where $\vec{p}^2/2m$ is the kinetic energy, V_ν is the contribution to perfect crystal potential due to the ν_{th} ion at $\vec{R}_\nu$, and V_p describes the polarization effect. The Hamiltonian for the region inside the cavity ($r<R$) has the form

$$H_< = \vec{p}^2/2m + V_0 + W_0\ .$$

The term V_0 is the spherically symmetric part of the point-ion crystal potential for the region $r \leq r_1$:

$$V_0 = Z_v Z_F\{(\alpha_M/r_1) + [S_1, Q_1, \sigma/r_1(1-\sigma)\}\ . \tag{8}$$

The quantity α_M is the Madelung potential constant at the anion site, S_i is the number of ions on the ith shell centered about the vacancy, and Q_i is the charge on one of the ions in the ith shell. The energy W_0 contains many terms which will be discussed below. Although the spherically symmetric part of the potential $\sum_\nu' V_\nu$ is used, this procedure is exact for matrix elements involving $1s$-, $2s$-, and $2p$-type wave functions which experience potentials having at least tetrahedral symmetry or higher. The procedure is not exact for d- or f-type wave functions. The Hamiltonian outside ($r>R$) the cavity has the form

$$H_> = (\vec{p}^2/2m) + \sum_\nu V_\nu(\vec{r}-\vec{R}_\nu) + V_p(\vec{r}) - V_0(\vec{r}) + V_{sf} + V_{sv}\ . \tag{9}$$

The F-electron and vacancy self-energies are denoted by V_{sf} and V_{sv}, respectively. The term $V_0(\vec{r})$ has been added and subtracted in Eq. (9). This procedure enables us to introduce the effective-mass approximation for which the terms $\vec{p}^2/2m + \sum_\nu V_\nu$ are replaced with the term $\vec{p}^2/2m^*$. The quantity m is the bare electron mass and the quantity m^* is the effective electron mass at the bottom of the conduction band. The effective mass is assumed to be a scalar. The terms $V_p(\vec{r}) - V_0(\vec{r})$ are written in a form containing a spatially dependent effective dielectric function $\epsilon_{eff}(r)$, which is assumed to be a function of only $r = |\vec{r}|$,

$$V_p(\vec{r}) - V_0(\vec{r}) = V_{F\text{-}V}(\vec{r}) \approx [Z_F Z_v/\epsilon_{eff}(r) r]\ . \tag{10}$$

The potential $V_{F\text{-}V}(r)$ represents the effective interaction between the F electron and an infinite mass hole (a vacancy) of charge Z_v due to the ionic polarizations. When the F electron is in a compact state (small orbit) or moves very rapidly, then one expects that $\epsilon_{eff} \approx \epsilon_\infty$. Also, when the F electron is in a diffuse state (large orbit) or moves so slowly that the ionic polarization can follow to some extent the electronic motion, one expects that $\epsilon_{eff} \approx \epsilon_0$. Hence, the potential $V_{F\text{-}V}(r)$ acts as an interpolation between the two extreme cases. Fowler[13] has extended Haken's theory[6] to obtain an approximate form for $V_{F\text{-}V}(r)$. Because the F center in systems for which the vacancy has an effective charge $Z_v = -Z_0$ greater than $+e$ (e.g., the oxides) also will be discussed, the above theories have been generalized mathematically[22] to treat the case of a mobile electron of charge Z_F in the presence of ionic polarizations. The results are

$$V_{sv} = -(Z_v^2/r_1)(\epsilon_\infty^{-1} - \epsilon_0^{-1})\ , \tag{11}$$

$$V_{sf} = -(Z_F^2/2)v(\epsilon_\infty^{-1} - \epsilon_0^{-1})\ , \tag{12}$$

and

$$V_{F\text{-}V}(r) \mp (Z_v Z_F/r)\{\epsilon_\infty^{-1} + (\epsilon_0^{-1} - \epsilon_\infty^{-1}) \times [1 - \tfrac{1}{2}(e^{-vr} + e^{-2r/r_1})]\}\ . \tag{13}$$

Here, $v = (2m^*\omega_l/\hbar)^{1/2}$ and ω_l is the frequency of the longitudinal-optical phonon for the crystal.

Expression (13) is valid only for the large values of r,

$$(Z_F^2/r)(\epsilon_\infty^{-1} - \epsilon_0^{-1}) < \hbar\omega_l\ . \tag{14}$$

However, Feynman[23] has shown that expression (13) is in a fact a qualitative interpolation between large and small r and is quantitatively correct up to order $[(1/r) + \text{const}]$ in the $r \to 0$ limit:

$$\lim_{r\to 0} V_{F\text{-}V}(r) = (Z_F Z_v/r\,\epsilon_\infty) - Z_F Z_v(\epsilon_\infty^{-1} - \epsilon_0^{-1})[(v/2) + (1/r_1)]\ . \tag{15}$$

The negative self-energy terms outside the cavity are equivalent to positive self-energy terms inside the cavity and a change in the zero of energy, namely,

$$\int_R^\infty r^2 dr \int d\Omega\, |\psi_\eta|^2 (V_{sv} + V_{sf}) = E_{SE} - \int_0^R r^2 dr \int d\Omega\, |\psi_\eta|^2 (V_{sv} + V_{sf})\ . \tag{16}$$

The change in the zero of energy from which the energy is measured is $E_{SE} = V_{sv} + V_{sf}$. This change is a constant and hence it is of no consequence.

The several terms contained in the second term

W_0 of the well depth, $V_\sigma + W_0$, are given now. Let us write

$$W_0 = -\chi + W_{\text{inf}} + W_{\text{opt}} ,$$

where χ is the energy at the bottom of the conduction band relative to the vacuum, where W_{inf} is the self-energy of the vacancy and F electron due to ionic polarizations, and where W_{opt} is the potential energy due to electronic polarizations. The self-energy due to ionic polarization becomes

$$W_{\text{inf}} = -(V_{sv} + V_{sf}) . \tag{17}$$

The location of the conduction band enters because the operator $\vec{p}^2/m + \sum_\nu V_\nu$ has the vacuum as the zero of energy and the operator $\vec{p}^2/2m^*$ has the bottom of the conduction band as the zero of energy. The self-energy of the F electron due to the optical polarization is not included explicitly because the quantity χ contains this term whenever experimentally determined values for χ are used.

Two expressions exist for the potential energy of the F electron due to the optical polarization when the F electron is in the cavity; the quasiadiabatic approximation[24] gives

$$W_{\text{opt}}(\text{QA}) = -(1 - \epsilon_\infty^{-1})[Z_v - (e/2)](Z_F/R) , \tag{18}$$

and the continuum Hartree approximation gives

$$W_{\text{opt}}(\text{HF}) = -(1 - \epsilon_\infty^{-1})(Z_F/R) \times [Z_v - e - Z_F R \int_R^\infty q(t) t^{-2} dt] , \tag{19}$$

where

$$q(t) = \int_t^\infty |\psi_\eta|^2 d^3u . \tag{20}$$

The adiabatic approximation allows the core dipoles to follow to some extent the motion of the F electron when the lattice is in the cavity; while the continuum Hartree approximation asserts that the core dipoles do not follow the F electron and that they point towards the mean position of the F electron when it is in the cavity.

The F electron experiences in the above theory a constant potential inside the cavity. More refined treatments are expected to lead to spatially dependent potentials for distances less than the nn distance. But the functional dependence of the constant well depth potential upon the F-electron wave function changes among the several approaches to the F center. Hence, any conclusions which obtain from any of these treatments of the F center are subject to the validity of a constant potential inside the cavity.

The five models which have been examined by numerical methods are given below.

A. SP(HF)

The SP(HF) Hamiltonian from which both the absorption and emission states are computed has the form

$$H_F(\text{HF}) = \begin{cases} H_<(\text{HF}) & \text{for } r \le R \\ H_>(\text{HF}) & \text{for } r > R , \end{cases} \tag{21}$$

where

$$H_<(\text{HF}) = \vec{p}^2/2m + V_0 - \chi + W_{\text{inf}} + W_{\text{opt}}(\text{HF}) \tag{22}$$

and

$$H_> = \vec{p}^2/2m^* + V_{F\text{-}V}(r) . \tag{23}$$

B. SP(QA)

The SP(QA) Hamiltonian from which both the absorption and emission states are computed has the form

$$H_F(\text{QA}) = \begin{cases} H_<(\text{QA}) & \text{for } r \le R \\ H_> & \text{for } r > R , \end{cases} \tag{24}$$

where

$$H_<(\text{QA}) = \vec{p}^2/2m + V_0 - \chi + W_{\text{inf}} + W_{\text{opt}}(\text{QA}) , \tag{25}$$

and where $H_>$ is given by Eq. (23).

C. SP(HF_1)

The remaining models are modifications of the SCP(HF) and SCP(QA) models. The motivation for developing these modifications arises in part from the need to reduce the computer time. But more importantly they arise from the necessity to treat the distant ionic polarizations for emission more realistically. Also, the SP(HF) and SP(QA) models cannot explain the Stark-effect experiments on F centers in KCl.

Use of the interaction $V_{F\text{-}V}(r)$ and its associated self-energy term W_{inf}, as they stand, may lead to subtle difficulties in the calculations for some F-center states. This interaction states that the ionic polarization of the lattice changes as the spatial extent of the F-electron wave function changes. The cases for which $Z_v = +e$ are examined first. The F-electron wave function, $\Psi_0(r) = \langle r | F_0^*; \sigma_0 \rangle$, for the relaxed ground state is most likely very well confined to the vacancy (spatially compact). The major contribution to the F-electron energy then comes from the term $H_<$ for the inside of the cavity and the term $V_{F\text{-}V}(r)$ in $H_>$ plays only a minor role. Hence, because the screening of the vacancy by a compact F-electron wave function beyond the nn ions is nearly complete, the terms $V_{F\text{-}V}(r)$ and W_{inf} may be set equal to zero. The effects of the ionic polarization and the nn ions are included, however, in the term V_0. Therefore, if the distant ionic polarization is assumed to be zero in the state $|F_0^*; \sigma_0\rangle$, then in accordance with the Franck-Condon principle it also should be zero in the final state of an optical-absorption transition, $|F_\eta; \sigma_0\rangle$. If the Franck-Condon principle were slightly violated during absorption, then small contributions from $V_{F\text{-}V}(r)$ and W_{inf} would have to be considered. However, the forms given by Eqs. (11)–(13) and the value of v used here

would lead to large ionic polarizations. It is not likely that large ionic polarizations develop during an optical-absorption process to even a diffuse excited state.[20] Therefore, in both the SP(HF_1) and SP(QA_1) models, for which $Z_v = +e$, the distant ionic polarization is zero for all states involved in the absorption process.

There does not appear to be any completely satisfactory way to treat the distant ionic polarization for the F-center states involved in emission.[20] Many models predict that the initial relaxed excited state of the emission process is spatially diffuse. These same models give conflicting results as to whether the final unrelaxed state in emission is compact or diffuse. Fowler[13] has suggested that an effective dielectric constant ϵ_{eff}, having a value between the high frequency ϵ_∞ and static ϵ_0 limits, can characterize reasonably well the distant ionic polarization for the states involved in emission. As the spatial extent of the F-electron state increases, the effective dielectric constant ϵ_{eff} approaches ϵ_0. The importance of $H_>$ also increases as the F-electron wave function becomes more diffuse. Under the above circumstance, the interaction potential is approximated when $Z_v = +e$ by

$$V_{F\text{-}V}(r) \approx (Z_v Z_F / \epsilon_{eff}\, r) \quad \text{for } r > R \,. \tag{26}$$

Fowler[13] and Wood and Öpik[20] cite ways to determine ϵ_{eff} approximately. The following method is used here. The effective-mass theory probably gives fairly accurate values for the energies of those relaxed excited states which lie near the conduction band. The energies of shallow hydrogeniclike states is given by

$$E - E_c = -(m^*/n^2 \epsilon_{eff}^2)(0.5 \text{ a.u.}) \,, \tag{27}$$

where E_c is the energy of the bottom of the conduction band. Setting $n = 2$ for an excited state and $E - E_c$ equal to the experimental value for the thermal ionization energy of the excited state gives by Eq. (27) an estimate for ϵ_{eff}. The final state of an emission process is assumed to obey strictly the Franck-Condon principle for the distant ionic polarization. The ionic polarization of the nn ions is treated explicitly in the term V_0.

The above discussions on the polarizations for absorption and emission when $Z_v = +e$ are extended now to the cases for which $Z_v \geq 2e$, e.g., the oxides. The effective vacancy charge is considered to be composed of an uncompensated charge $(Z_v - e)$ and of a charge $+e$ which is essentially compensated by a compact F-electron wave function. The potentials arising from the ionic and electronic polarizations induced by the uncompensated charge $(Z_v - e)$ are the same for all states and are, respectively, for $r > R$,

$$V_{i,\mathrm{uc}}(r) = [Z_F(Z_v - e)/r]\,(\epsilon_0^{-1} - \epsilon_\infty^{-1}) \tag{28}$$

and

$$V_{e,\mathrm{uc}}(r) = [Z_F(Z_v - e)/\epsilon_{eff}\, r] \,. \tag{29}$$

The potential arising from the ionic polarization induced by the partially compensated charge $+e$ depends upon the state. It is zero for absorption states and it is approximated for emission states by

$$V_{i,c}(\mathrm{ems}, r) = (Z_F\, e/r)(\epsilon_{eff}^{-1} - \epsilon_\infty^{-1}) \,, \tag{30}$$

where $r > R$. The electronic polarization induced by the partially compensated charge $+e$ gives a potential for $r > R$,

$$V_{e,c}(r) = (Z_F\, e/\epsilon_\infty\, r) \,. \tag{31}$$

Observe that the terms $V_{i,\mathrm{uc}}$ and $V_{e,\mathrm{uc}}$ are zero for the alkali halides.

The above potentials are used now to state the Hamiltonian for the SP(HF_1) model. The SP(HF_1) Hamiltonian is given by the following relations:

$$H_F(\mathrm{HF}_1) = \begin{cases} H_<(\mathrm{HF}_1) & \text{for } r \leq R \\ H_>(\mathrm{HF}_1) & \text{for } r > R \,, \end{cases} \tag{32}$$

where for those states involved in an *absorption process*

$$H_<(\mathrm{HF}_1) = \vec{p}^{\,2}/2m + V_0 - \chi + W_{opt}(\mathrm{HF}) \tag{33}$$

and

$$H_>(\mathrm{HF}_1) = \vec{p}^{\,2}/2m^* + V_{i,\mathrm{uc}}(r) + V_{e,\mathrm{uc}}(r) + V_{e,c}(r) \,, \tag{34}$$

and where for states involved in an *emission process*

$$H_<(\mathrm{HF}_1) = \vec{p}^{\,2}/2m + V_0 - \chi + W_{opt}\,\mathrm{HF} \tag{35}$$

and

$$H_>(\mathrm{HF}_1) = \vec{p}^{\,2}/2m^* + V_{i,\mathrm{uc}}(r) + V_{e,\mathrm{uc}}(r) + V_{e,c}(r) + V_{i,c}(\mathrm{ems}, r) \,. \tag{36}$$

The self-energies associated with the uncompensated charge are included in the lattice energy $H_L(\vec{R})$ and hence does not appear in the above expressions.

D. SP(QA_1)

The SP(QA_1) Hamiltonians for the absorption and emission states are, except for one term, the same as those for the SCP(HF_1) Hamiltonians. The one exception is that the term W_{opt} (HF) in Eqs. (33) and (35) is replaced by the term W_{opt}(QA).

E. SP(EI_1)

The SP(EI_1) model incorporates the forms for the ionic and electronic polarizations suggested by Toyozawa[25] and Haken and Schottky[26] in their works on Wannier excitons. In addition to the potentials and self-energies for the ionic polarizations [$V_{F\text{-}V}(r)$, V_{sv}, and V_{sf}; Eqs. (11), (12), and (13)], functionally similar forms are introduced to replace

the potentials for electronic polarizations, i.e., the terms $V_{e,c}(r)$ and W_{opt}. The polarization potential due to the distortion of the electronic orbitals is given by[20]

$$U_{F\text{-}V}(r) = (Z_F Z_v/r)\{1 + (\epsilon_\infty^{-1} - 1) \times [1 - \tfrac{1}{2}(e^{-\rho_e r} + e^{-\rho_h r})]\}, \quad (37)$$

where $\rho_e = \rho_h = R^{-1}$. The associated self-energy is

$$U_{opt} = \tfrac{1}{2}[(Z_v^2/R) + (Z_F^2/R)](\epsilon_\infty^{-1} - 1).$$

Applying the same assumptions for the absorption and emission states as those for the SP(HF_1) and SP(QA_1) models gives the following Hamiltonian for the SP(E_1) model:

$$H_F(EI_1) = \begin{cases} H_<(EI_1) & \text{for } r \leq R \\ H_>(EI_1) & \text{for } r > R, \end{cases} \quad (38)$$

where for *absorption* processes,

$$H_<(EI_1) = \vec{p}^{\,2}/2m + V_0 - \chi + U_{opt} \quad (39)$$

and

$$H_>(EI_1) = \vec{p}^{\,2}/2m^* + V_{i,uc}(r) + U_{F\text{-}V}(r), \quad (40)$$

and where for *emission* processes,

$$H_<(EI_1) = \vec{p}^{\,2}/2m + V_0 - \chi + W_{inf} + U_{opt} \quad (41)$$

and

$$H_>(EI_1) = \vec{p}^{\,2}/2m^* + V_{i,uc}(r) + V_{i,c}(\text{ems}, r) + U_{F\text{-}V}(r). \quad (42)$$

The value for χ used in Eqs. (39) and (41) should not include the self-energy of the F electron due to the optical polarization.

IV. POLARIZABLE-ION MODELS

The exact solutions to the PI(2) model of Ref. 8 require excessive amounts of computer time. A simplified version of this model [PI(3) model] is presented here.

The kinetic-energy operator is simply $\vec{p}^{\,2}/2m$. The ions are considered as point charges Z_ν. The F-electron–point-ion interaction is written then in the form

$$H_2(\vec{r}, \sigma) = Z_F \sum_{\nu \neq 0}{}' \frac{Z_\nu}{|\vec{r} - \vec{r}_\nu|}, \quad (43)$$

where the prime means that the $\nu = 0$ site is excluded from the summation, and $\vec{r}_\nu$ is the location of the νth ion. The Madelung constant is defined by

$$\alpha_M = \bar{r}_1 H_2(0, 0) Z_F^{-1},$$

where $\bar{r}_1$ is the nn distance (anion-cation) for the NaCl structure and is the lattice constant (cation-cation) for the CaF_2 structure.

Because the F-electron wave functions shall be limited to 1s-, 2s-, and 2p-like functions, it is necessary to consider only the spherically symmetric part of $H_2(\vec{r}, \sigma)$.[8] The spherically symmetric part of $H_2(\vec{r}, \sigma)$ is denoted by $V_{sph}(\vec{r}, \sigma)$. The point ions are distributed on shells centered at the anion vacancy. The radius of shell n is denoted by r_n, the number of ions on shell n by S_n, and the charge of the νth ion on shell n by $Q_n = Z_\nu$. The spherically symmetric part of the crystal potential $V_{sph}(\vec{r}, \sigma)$ is expressed in terms of the above notation, namely,

$$V_{sph}(\vec{r}, \sigma) = \begin{cases} V_0 & \text{for } 0 < r < r_1' \\ V_0 - [(S_1 Q_1/r_1') - (S_1 Q_1/r_1)] Z_v Z_F & \\ \qquad \text{for } r_1' < r < r_2 & \\ V_n + (D_n/r) & \text{for } r_n < r < r_{nH}, \end{cases}$$

where for $n \geq 2$,

$$V_n = V_0 - Z_v Z_F \left(\frac{S_1 Q_1}{r_1'} + \sum_{i=2}^{n} \frac{S_i Q_i}{r_i} \right)$$

and

$$D_n = Z_v Z_F \sum_{i=1}^{n} S_i Q_i .$$

The term $[S_1 Q_1 \sigma / r_1 (1 - \sigma)]$ in V_0 represents the total ionic polarization potential arising from the first shell and includes the effects of both the point charge Z_v and the F electron. Because practical considerations limit the number of shells which are treated explicitly, the first 21 shells are considered in our computations. The Coulomb potential

$$V_{sph}(r) = (Z_v Z_F/r) \quad \text{for } r > r_{21},$$

is used for distances beyond the 21st shell.

The Hamiltonian for the PI(3) model then becomes simply

$$H_F(\text{PI}) = \begin{cases} \vec{p}^{\,2}/2m + V_0 & \text{for } r \leq r_1' \\ \vec{p}^{\,2}/2m + V_{sph}(\vec{r}, \sigma) & \text{for } r > r_1'. \end{cases}$$

V. ABSORPTION AND EMISSION

The initial state of an optical transition is a relaxed state $|F_i^*; \sigma_i\rangle$. The total F-center energy $E_T(\eta_i; \sigma) = \langle F_i^*; \sigma | H_T | F_i^*; \sigma \rangle$ is minimized with respect to the nn ionic polarization σ to obtain the energy of the initial state $E_i = E_T(\eta_i; \sigma)$. The value σ_i is that value of σ for which $E_T(\eta_i; \sigma)$ attains its minimum value. The F center then undergoes an optical transition to the state $|F_f; \sigma_i\rangle$, which is assumed to be a quasistationary state with an electronic wave function calculated for the same distortion σ_i as that for the initial state $|F_i^*; \sigma_i\rangle$. This is a statement of the Franck-Condon principle. The distortion σ represents the ionic displacement of the nn ions due to both the F electron and the effective vacancy charge Z_v. The total energy of the final state is $E_f = E_T(\eta_f; \sigma_i)$. The optical-absorption energy is denoted by

$$E_{if}(\text{abs}) = E_T(\eta_f; \sigma_i^a) - E_T(\eta_i; \sigma_i^a), \tag{44}$$

and the optical-emission energy is denoted by

$$E_{if}(\text{ems}) = E_T(\eta_i; \sigma_i^e) - E_T(\eta_f; \sigma_i^e). \tag{45}$$

Each term on the right-hand side of Eqs. (44) and (45) is a negative number. Also, the ionic displacement for absorption σ_i^a in Eq. (44) differs from the ionic displacement for emission σ_i^e in Eq. (45).

The expectation value of a given power of the radial coordinate r gives us information on the spatial extent of the F-electron wave function. The first and third powers of r are chosen to indicate the spatial extent, namely,

$$r(n; \eta; \sigma) = r_1^{-n} \int R_\eta(r)\, r^n R_\eta(r)\, 4\pi r^2 dr; \tag{46}$$

where $R_\eta(r)$ is the radial part of $\psi_\eta(r)$ and $n = 1$ or $n = 3$.

A bound state is considered compact for values of $r(1; \eta; \sigma) \lesssim 1$ and diffuse for values of $r(1, \eta, \sigma) \gtrsim 3$. For values between 1 and 3 the decision is rather subjective. The ratio $r_e(\eta; \sigma) = [r(3; \eta; \sigma)/r_1^2 r(1; \eta; \sigma)]$ also indicates to what extent the radial functions have extended tails. Values of $r_e < 1$ indicate compact states and values of $r_e > 1$ indicate diffuse states. The author has chosen to present the wave-function data in this manner and not to present many numerical tables of the wave functions as functions of the radial coordinate.

The lifetime of the relaxed excited state $|F_1^*; \sigma_1\rangle$ is proportional to the ratio of the square of the dipole matrix elements for absorption and for emission. An estimate for the radiative lifetime is given by[7]

$$\tau = \tau_R \times 10^{-7} \text{ sec},$$

where

$$\tau_R = \frac{|\langle F_1; \sigma_0 | z | F_0^*; \sigma_0 \rangle_{\text{abs}}|^2}{|\langle F_0; \sigma_1 | z | F_1^*; \sigma_1 \rangle_{\text{ems}}|^2}. \tag{47}$$

Only dipole radiation is considered in the above estimate for the radiative lifetime. There are, of course, other processes which may compete with the dipole-radiation decay. These are nonradiative decay (high-temperature thermal ionization) of the excited state and tunneling to the conduction band. Hence, the present treatment of F-center models are least subject to criticism for low temperatures.

VI. RESULTS

In this section, the results of the preceding models are reported and are compared with the past results from Refs. 7 and 8. The presentation includes the predictions of the above six models for KCl, CaO, and CaF_2. The Born-Mayer empirical form [Eq. (15) of Ref. 7] for the repulsive energy terms is used. Table I contains the values of the input data for the six models.

The $|1s; \sigma\rangle$, $|2s; \sigma\rangle$, and $|2p; \sigma\rangle$ F-center states for the six preceding models have been determined exactly by numerical methods. The absorption energy, the emission energy, and the lifetime of the relaxed $|2p; \sigma_1\rangle$ state are given in Tables II–IV for each model and for KCl, CaO, and CaF_2. Comparisons with the variational methods of Refs. 7 and 8 are given also in these tables. The presence of the $|2s; \sigma\rangle$ state is neglected in the calculations for Tables II–IV.

Among the absorption energy, the emission energy, and the lifetime, the lifetime is most sensitive to the details of a given model. If the lifetime is known, it should be given more weight for a decision on a model's worth than the less-model-sensitive absorption and emission energies.

The theoretical estimates for the lifetimes are computed from Eq. (47) by setting

$$|F_0^*; \sigma_0\rangle = |1s; \sigma_0\rangle, \qquad |F_1; \sigma_0\rangle = |2p; \sigma_0\rangle,$$
$$|F_1^*; \sigma_1\rangle = |2p; \sigma_1\rangle, \qquad |F_0; \sigma_1\rangle = |1s; \sigma_1\rangle.$$

The results are quoted in Table II. Table II for KCl shows that none of the exact solutions explain the long lifetime, although the SP(HF) and SP(HF) exact) models agree reasonably well with the experimental absorption and emission energies. The $SP(HF_1)$ model agrees best among the exact-solution models and its lifetime is a factor of 3 too small.

Decisions as to which model in Table III is best for CaO and as to which model in Table IV is best for CaF_2 are less certain than the decision for KCl. Present experimental data lead one to conclude that the exact solutions to the PI(3) models for CaO and CaF_2 agree best with experiment and have the greatest promise for additional improvement. The exact solutions to all the SP models predict very large Stoke's shifts for CaO and CaF_2. Such results are questionable. This statement about SP models for F centers in CaO is consistent with the remarks of caution, given in Sec. IV of Ref. 7, on applying SP models to CaO.

Tables V–VII contain, respectively, more detailed results predicted by the $SP(HF_1)$ model for KCl and by the PI(3) models for CaO and CaF_2. Observe that the $|1s; \sigma_0\rangle$ state is usually the only state which has a compact F-electron wave function and that the $|2p; \sigma_1\rangle$ and $|2s; \sigma_1\rangle$ states lie close together in the $SP(HF_1)$ model for KCl in emission. These observations agree with those of Refs. 16 and 18.

VII. INTERNAL STARK EFFECT IN KCl

It is shown in this section that a mechanism which sufficiently mixes the $|2p; \sigma_1\rangle$ and $|2s; \sigma_1\rangle$ states can account for the long lifetime of the re-

TABLE I. Input data for F-center models. The Pauling factor for the ith and jth ions is β_{ij}. The ionic radius of the cation is ρ_+ and of the anion is ρ_-. The quantity ρ is the stiffness factor in the empirical Born-Mayer exponential form which characterizes the repulsive energy between the ith and jth ions. The Madelung potential constant at the anion site is α_M. The high-frequency, low-frequency, and effective dielectric constants are ϵ_∞, ϵ_0, and ϵ_{eff}, respectively. The longitudinal optical phonon frequency ω_l is expressed in units of 10^{13} rad sec^{-1}. The Mott-Littleton radius R is given by $R = r_1(1 - d_{ML})$. The quantity $\bar{r}_1$ is the nn distance (anion-cation) for the NaCl structure and is the lattice constant (cation-cation) for the CaF_2 structure. The series coefficients C_4, C_6, and C_8 appear in the expansion in powers of the lattice distortion σ for the change in electrostatic energy E_1 which occurs when a cation moves in the background of a perfect point-ion lattice potential, namely, $E_1 = -(6/\bar{r}_1)(C_4\sigma^4 + C_6\sigma^6 + C_8\sigma^8)$. The energy at the bottom of the conduction band relative to an electron at rest infinitely far from the F center is χ. The quantity m is the bare electron mass and the quantity m^* is the effective mass at the bottom of the conduction band. The quantities β_{++}, β_{+-}, β_{--}, α_M, ϵ_∞^{-1}, ϵ_0^{-1}, ϵ_{eff}^{-1}, d_{ML}, and m^*/m are dimensionless. All other quantities are expressed in terms of atomic units (1 a. u. = 27.2 eV for energy and 0.529×10^{-8} cm for length).

	KCl	CaO	CaF_2
β_{++}	1.25	1.50	1.50
β_{+-}	1.00	1.00	1.125
β_{--}	0.75	0.50	0.75
ρ_+	2.77[a]	2.21[b]	2.21[c]
ρ_-	3.00[a]	2.55[b]	1.98[c]
ρ	0.637[a]	0.629[b]	0.546[d]
α_M	1.748	1.748	4.071
ϵ_∞^{-1}	0.469[e]	0.305[e]	0.489[f]
ϵ_0^{-1}	0.214[e]	0.085[e]	0.149[f]
ϵ_{eff}^{-1}	0.258	0.200	0.250
ω_l	3.95[e]	13.07[e]	1.38[e]
d_{ML}	0.140[g]	0.120[g]	0.074[d]
$\bar{r}_1$	5.93[a]	4.54[b]	10.32[c]
C_4	3.579[h]	3.579[h]	1.865[i]
C_6	0.9895[h]	0.9895[h]	...
C_8	2.942[h]	2.942[h]	...
χ	−0.022[j]	k	k
m^*/m	0.6[l]	k	k

[a]M. P. Tosi, in *Solid State Physics*, edited by F. Seitz and D. Turnbull (Academic, New York, 1964), Vol. XVI, p. 52.

[b]M. L. Huggins and Y. Sakamoto, J. Phys. Soc. (Japan) 12, 241 (1957).

[c]G. C. Benson and E. Dempsey, Proc. Roy. Soc. (London) A266, 344 (1962).

[d]A. D. Franklin (private communication).

[e]M. Born and K. Huang, *Dynamical Theory of Crystal Lattices* (Oxford U. P., Oxford, England, 1954), p. 85, Table 17.

[f]W. Kaiser *et al.*, Phys. Rev. 127, 1950 (1962).

[g]F. K. du Pré, J. Chem. Phys. 18, 379 (1950).

[h]A. Scholz, Phys. Status Solidi 7, 973 (1964).

[i]H. S. Bennett, J. Res. Natl. Bur. Std. 72A, 471 (1968).

[j]T. Timusk and W. Martienssen, Phys. Rev. 128, 1656 (1962).

[k]The value of χ is assumed to be 0.04 a. u. for CaO and CaF_2; the value of m^*/m is assumed to be 1.0 for CaO and 0.6 for CaF_2.

[l]W. B. Fowler, Phys. Rev. 135, A1725 (1964).

TABLE II. Predictions of the exact solutions and approximate solutions to SP and PI models for KCl. The absorption energy is E(abs) and the emission energy is E(ems). An estimate for the theoretical lifetime of the relaxed $|2p;\sigma\rangle$ state is $\tau_R \times 10^{-7}$ sec and the experimental lifetime of the state $|F^*\rangle$ is τ_R(expt) $\times 10^{-7}$ sec. The presence of the 2s-like state is neglected in the theoretical results of this table. The notation "exact" refers to the exact numerical solutions to a model and the notation "approx." refers to the approximate variational solutions given in Refs. 7 or 8 to a model. If the notation "exact" or "approx" does not appear in a model designator, then the predictions of the model are based upon the exact numerical solutions to that model. The energies are in atomic units.

	KCl		
Model	E(abs)	E(ems)	τ_R
Experiment	0.085[a]	0.046[a]	5.71[a]
SP(HF_1)	0.109	0.045	1.90
SP(HF, exact)	0.111	0.045	1.09
SP(HF, approx)	0.102	0.045	8.39
SP(QA_1)	0.083	0.023	0.76
SP(QA, exact)	0.066	0.026	0.41
SP(EI_1)	0.046	0.015	0.38
PI(2, approx)	0.086	0.074	0.87
PI(3)	0.078	0.072	0.92

[a]J. J. Makhan, in *Solid State Physics*, edited by F. Seitz and D. Turnbull (Academic, New York, 1966), Vol. VIII Suppl., Tables 3.2a, 8.1, and 8.5.

laxed excited state $|F^*\rangle$ in KCl. One possible mixing mechanism arises from the fluctuating internal electric fields of noncubic longitudinal-optical phonons moving through the F center. These fluctuating fields produce under the proper conditions an effective electric field at the F center. If a given F-center state exists for a long enough time compared to the period of the noncubic phonon, then the F electron in such a state responds adiabatically and experiences a nonzero electric field (internal Stark effect). The exact nature of this mechanism is difficult at present to determine.

TABLE III. Predictions of the exact and approximate solutions to SP and PI models for CaO. The notation is the same as that for Table II.

Model	E(abs)	E(ems)	τ_R
Experiment	0.134[a]	0.121[a]	b
PI(3)	0.124	0.121	0.98
PI(2, approx)	0.127	0.119	~0.90
SP(HE_1)	0.170	0.008	0.05
SP(HF, exact)	0.075	0.011	0.03
SP(QA_1)	0.137	0.009	0.08
SP(QA, exact)	0.013	0.012	0.83
SP(EI_1)	0.041	0.016	0.41

[a]J. C. Kemp *et al.*, Phys. Rev. 171, 1024 (1968); B. D. Evans *et al.*, Phys. Letters 27A, 506 (1968).

[b]Experimental values have not been reported.

TABLE IV. Predictions of the exact and approximate solutions to SP and PI models for CaF_2. The notation is the same as that for Table II.

Model	E(abs)	E(ems)	τ_R
Experiment	0.121[a]	b	b
PI(3)	0.131	0.113	0.87
PI(2, approx)	0.142	0.125	0.86
SP(HF_1)	0.169	0.022	0.48
SP(HF, exact)	0.103	0.027	0.05
SP(HF, approx)	0.120	...	...
SP(QA_1)	0.129	0.016	0.26
SP(QA, exact)	0.76	0.020	0.10
SP(EI_1)	0.072	0.013	0.20

[a]P. Feltham and I. Anders, Phys. Status Solidi 10, 203 (1965), Table 3.

[b]Experimental values have not been reported.

Additional research is required in order to have a better understanding of such mechanisms.

It shall be asserted in this paper that as the lifetime of a state increases the internal Stark effect due to noncubic phonons becomes more important. This is the case for the F center in KCl. Because the unrelaxed excited states have relatively short lifetimes compared to the relaxed excited states in KCl, the internal Stark effect is negligible for the F-center states associated with absorption. In addition, because the spacings among the energies for the $1s$-, $2p$-, and $2s$-like states are greater in absorption than they are in emission, the Stark effect is substantially less for absorption than it is for emission. The internal Stark effect is considered then only for the F-center states associated with the emission process.

Let us assume that the noncubic longitudinal-optical phonons produce in the z direction an effective nonzero electric field over a volume comparable to the spatial extent of the F-electron wave function for the state $|F^*\rangle$. That is, the internal electric field is $\vec{E}_{\rm int}(e) = E_s\hat{z}$ for emission. Whenever $E_s \neq 0$, then the degeneracy among the $|2p_x;\sigma_1\rangle$, $|2p_y;\sigma_1\rangle$, and $|2p_z;\sigma_1\rangle$ states is removed. The state $|2p_z;\sigma_1\rangle$ then has an energy which differs from the energy of the remaining degenerate pair of states $|2p_x;\sigma_1\rangle$ and $|2p_y;\sigma_1\rangle$.

The internal Stark effect is computed now for the subset of states $|2p_z;\sigma_1\rangle$ and $|2s;\sigma_1\rangle$. The F center in the presence of the internal field is described by the Hamiltonian[27]

$$H_s = H_T - eE_s z . \tag{48}$$

The following notation is introduced for convenience:

$$\epsilon_\eta = E_T(\eta;\sigma_1), \qquad \delta_\eta = \epsilon_\eta - \epsilon_{2p_z},$$
$$D_\eta = \langle \eta;\sigma_1 | z | 2p_z;\sigma_1\rangle, \qquad \epsilon = (\delta_{2s}/2eE_sD_{2s}),$$

where $D_{2s} > 0$. Solving the secular equations for the Hamiltonian, Eq. (48), gives the admixed states $|F_+^*;\sigma_1\rangle$ and $|F_-^*;\sigma_1\rangle$ and their respective energies E_+ and E_-, namely,

$$|F_+^*;\sigma_1\rangle = M|2p_z;\sigma_1\rangle + N|2s;\sigma_1\rangle,$$
$$|F_-^*;\sigma_1\rangle = N|2p_z;\sigma_1\rangle - M|2s;\sigma_1\rangle, \tag{49}$$

$$E_+ = \tfrac{1}{2}(\epsilon_{2s}+\epsilon_{2p}) + eE_sD_{2s},$$
$$E_- = \tfrac{1}{2}(\epsilon_{2s}+\epsilon_{2p}) - eE_sD_{2s}, \tag{50}$$

where

$$M^2 = \tfrac{1}{2}[1 \mp (1+\epsilon^{-2})^{-1/2}] \tag{51}$$

and

$$N^2 = \tfrac{1}{2}[1 \pm (1+\epsilon^{-2})^{-1/2}] . \tag{52}$$

The top signs refer to the case in which $\epsilon > 0$ and the bottom signs refer to the case in which $\epsilon < 0$.

The presence of the $|1s;\sigma_1\rangle$ state and other states lying above the $|2p;\sigma_1\rangle$ and $|2s;\sigma_1\rangle$ states has not been taken into account in deriving Eqs. (49) and (50). These equations therefore are valid physically only when $|\delta_{2s}| < |\epsilon_{2s}| < |\epsilon_{2p_z}|$, $|\delta_{2s}| < |\delta_\eta|$, $|D_{1s}| < |D_{2s}|$, and $|D_\eta| < |D_{2s}|$. All models studied, except the PI(3) model, satisfy these inequalities. Nonetheless, a computer program was written to compute the Stark effect for the subset of states $|1s;\sigma_1\rangle$, $|2p_z;\sigma_1\rangle$, and $|2s;\sigma_1\rangle$. The numerical results quoted at the end of this section are those given by the more refined computer treatment.

TABLE V. Low-lying states for the F center in KCl which are predicted by the exact numerical solutions to the SP(HF_1) model. The initial state is the relaxed $|\eta;\sigma\rangle$ state and the value of σ remains the same for the other states. The total energy of the state $|\eta;\sigma\rangle$ is E_T. The spatial extent quantities $r(1) = r(1;\eta;\sigma)$, $r(3) = r(3;\eta;\sigma)$, and $r_e = (\eta;\sigma)$ are dimensionless. The energies are expressed in terms of atomic units (1 a.u. = 27.2 eV).

State	$1s$	$2p$	$2s$
Initial relaxed state has $\eta = 1s$ and $\sigma = \sigma_0 = 0.006$			
E_T	−0.165	−0.054	−0.016
$r(1)$	0.700	38.5	3.10
$r(3)$	0.595	224	44.3
r_e	0.821	58.2	14.3
Initial relaxed state has $\eta = 2p$ and $\sigma = \sigma_\perp = -0.100$			
E_T	−0.090	−0.045	−0.044
$r(1)$	1.03	5.45	6.86
$r(3)$	2.75	271	481
r_e	2.66	49.9	70.1
Initial relaxed state has $\eta = 2s$ and $\sigma = -0.096$			
E_T	...	−0.059	−0.056
$r(1)$	...	2.61	3.77
$r(3)$	...	61.2	77.8
r_e	...	23.5	20.6

TABLE VI. Low-lying states for the F center in CaO which are predicted by the exact numerical solutions to the PI(3) model. The notation in this table is the same as the notation given in Table V.

State	$1s$	$2p$	$2s$
Initial relaxed state has $\eta = 1s$ and $\sigma = \sigma_0 = -0.058$			
E_T	−0.678	−0.554	−0.392
$r(1)$	0.711	0.870	1.60
$r(3)$	0.520	0.856	6.11
r_e	0.732	0.984	3.81
Initial relaxed state has $\eta = 2p$ and $\sigma = \sigma_1 = -0.068$			
E_T	−0.677	−0.555	−0.407
$r(1)$	0.718	0.882	1.69
$r(3)$	0.538	0.902	6.76
r_e	0.749	1.02	4.00
Initial relaxed state has $\eta = 2s$ and $\sigma = -0.119$			
E_T	···	−0.521	−0.446
$r(1)$	···	1.00	1.91
$r(3)$	···	1.49	8.68
r_e	···	1.49	4.54

Except for the PI(3) model, very little $1s$ character appears in the low-lying excited states and very little $2p$ character and $2s$ character appear in the final state for emission $|F_0;\sigma_1\rangle$. The analytic solutions to the secular equations for the subset of states $|1s;\sigma_1\rangle$, $|2p_z;\sigma_1\rangle$, and $|2s;\sigma_1\rangle$ are not presented because they are very lengthy and because Eqs. (49) and (50) contain the important physical consequences of the internal Stark effect.

The dipole-radiation matrix element for emission from the $|F_-^*;\sigma_1\rangle$ state to the unrelaxed ground state $|F_0;\sigma_1\rangle \approx |1s;\sigma_1\rangle$ becomes

$$\langle F_0;\sigma_1|z|F_-^*;\sigma_1\rangle \approx ND_{1s}. \tag{53}$$

Replacing the matrix element for emission in Eq. (47) with Eq. (53) gives an expression for the lifetime of the state $|F_-^*;\sigma_1\rangle$, $\tau_{SR}(\epsilon)$ due to the admixture of $2p$- and $2s$-like states by the internal field $\vec{E}_{int}$:

$$\tau_{SR}(\epsilon) = N^{-2}\tau_R. \tag{54}$$

The physical statements contained in Eq. (54) are displayed more readily by expanding in powers of ϵ, when ϵ is small, and in powers of $1/|\epsilon|$, when ϵ is large. The respective expansions are as follows:

$$[\tau_{SR}(\epsilon)/\tau_R] \sim 2 - 2\epsilon + 2\epsilon^2 - \cdots \quad \text{for } |\epsilon| \ll 1, \tag{55}$$

$$[\tau_{SR}(\epsilon)/\tau_R] \sim 1 + (4\epsilon^2)^{-1} - (8\epsilon^4)^{-1} + \cdots \quad \text{for } \epsilon > 0 \text{ and } \epsilon \gg 1, \tag{56}$$

$$[\tau_{SR}(\epsilon)/\tau_R] \sim 4\epsilon^2 + 3 - (4\epsilon^2)^{-1} + \cdots \quad \text{for } \epsilon < 0 \text{ and } |\epsilon| \gg 1. \tag{57}$$

Equations (55) to (57) predict three physical consequences. Namely, when $\epsilon > 0$ (i.e., the $2p$ state lies lower than the $2s$ state), the predicted lifetime $\tau_{SR}(\epsilon)$ increases slowly from τ_R to $2\tau_R$ as the electric field E_s increases from 0 to ∞. Also, when $\epsilon < 0$ (i.e., the $2s$ state lies lower than the $2p$ state), the predicted lifetime $\tau_{SR}(\epsilon)$, decreases first rapidly from ∞ and then approaches slowly the value $2\tau_R$ as the electric field E_s increases from 0 to ∞. And when $\epsilon = 0$ (the $2p$ state and the $2s$ state are degenerate), the predicted lifetime is $2\tau_R$ and is independent of the electric field. In summary then, the above three statements indicate that precise measurements of the lifetime as a function of an applied electric field can be used to determine the relative locations of the $2p$- and $2s$-like states. Stiles *et al.* have made such measurements.[18] They find that the $2s$-like state lies 0.0006 a.u. below the $2p$-like state. This corresponds to a negative and small value for ϵ and to strong mixing of the $2p$- and $2s$-like states.

The exact results from each of the six models contained in Secs. III and IV are used to compute the internal Stark effect for the F center in KCl. The subset of states consisting of the three states $|1s;\sigma_1\rangle$, $|2p;\sigma_1\rangle$, and $|2s;\sigma_1\rangle$ for each model is included in these computations. Among the six models studied, the SP(HF_1) model for KCl yields a lifetime which is in best agreement with the experimental lifetime. When the internal electric field E_s is 10^7 V/m ($\epsilon \sim 0.25$) then the theoretical lifetime τ_{SR} is 3.1×10^{-7} sec. The experimental lifetime is 5.7×10^{-7} sec. The value of $\epsilon \sim 0.25$ also corresponds to a strong mixing of the $2p$- and

TABLE VII. Low-lying states for the F center in CaF_2 which are predicted by the exact solutions to the PI(3) model. The notation in this table is the same as the notation given in Table V.

State	$1s$	$2p$	$2s$
Initial relaxed state has $\eta = 1s$ and $\sigma = \sigma_0 = 0.037$			
E_T	−0.276	−0.145	−0.036
$r(1)$	0.701	0.897	2.05
$r(3)$	0.516	1.02	11.8
r_e	0.736	1.13	5.75
Initial relaxed state has $\eta = 2p$ and $\sigma = \sigma_1 = -0.008$			
E_T	−0.267	−0.154	−0.090
$r(1)$	0.751	1.02	2.17
$r(3)$	0.652	1.66	13.8
r_e	0.868	1.62	6.34
Initial relaxed state has $\eta = 2s$ and $\sigma = -0.070$			
E_T	···	−0.143	−0.120
$r(1)$	···	1.48	2.29
$r(3)$	···	5.19	16.6
r_e	···	3.51	7.26

$2s$-like states. In particular, the admixed states for $\epsilon \sim 0.25$ are

$$|F_-;\sigma_1\rangle \sim -0.788|2p;\sigma_1\rangle + 0.615|2s;\sigma_1\rangle,$$

$$|F_+;\sigma_1\rangle \sim +0.615|2p;\sigma_1\rangle + 0.788|2s;\sigma_1\rangle.$$

The shifts of the energy eigenvalues from $E_T(2p;\sigma_1)$ to ω_- and from $E_T(2s;\sigma_1)$ to ω_+ are less than both the mathematical accuracy and the physical accuracy of the model, i.e., $|E_T(2p;\sigma_1)-\omega_-| < 0.001$ a.u. and $|E_T(2s;\sigma_1)-\omega_+| < 0.001$ a.u. The unperturbed level separation is about 0.001 a.u.

The five remaining models all predict lifetimes which are less than 10^{-7} sec, even when the internal Stark effect is taken into account for electric fields as large as 10^{10} V/m. Intrinsic fields in ionic crystals are of the order of 10^{10} V/m. Fields larger than this would lead to catastrophic breakdown. Also, the electric fields used to determine dielectric constants and polarizabilities are usually about 10^3 V/m. Displacing the nn ion at $r_1\hat{z}$ to $(r_1+z)\hat{z}$ and the nn ion at $-r_1\hat{z}$ to $(-r_1+z)\hat{z}$ produces an electric field at the origin equal to 10^7 V/m when $z/r_1 \sim 1.7\times10^{-4}$. This dimensionless distortion is much less than the dimensionless distortion $\sigma_1 = -0.100$ for emission.

Hence, the SP(HF_1) model and the assumed internal Stark effect describe the relaxed excited state of the F center in KCl reasonably well. The only disagreement with recent experiments is the relative locations of the $2p$- and $2s$-like unperturbed states. This one point of disagreement is marginal, however, because the theoretical $2p$- and $2s$-level separation is comparable to the mathematical accuracy to which the model has been solved.

VIII. CONCLUSIONS

The three lowest-lying F-center states for KCl, CaO, and CaF_2 have been calculated within the framework of five SP models and one PI model. The exact solutions to the HFS equations for these six models have been obtained numerically. Both the initial and final states for the transitions of optical absorption and emission have been determined.

The SP(HF_1) model is the most successful model for the F center in KCl. When the internal Stark effect is computed from the unperturbed states $|1s;\sigma\rangle$, $|2p;\sigma\rangle$, and $|2s;\sigma\rangle$ predicted by this model, the agreement between theory and experiment is acceptable. Both theory and experiment suggest that the emission process for the F center in KCl can be interpreted in terms of a relaxed excited state which contains a strong mixture of $2p$- and $2s$-like unperturbed states. The recent experiments[16,18] are most consistent with the view that the $2s$-like state lies close to and lower than the $2p$-like state during the emission process. The present solutions, which are physically accurate to at most ±5% and mathematically accurate to ±0.1%, predict that the $2p$-like state lies close to and lower than the $2s$-like state during the emission process. The relative locations of the $2p$- and $2s$-like states should be considered with caution. An improvement in either the physical or mathematical accuracy of the SP(HF_1) could easily yield a $2s$ state being close to but lower than the $2p$ state. The important feature is the change in the angular character of the excited F-electron wave function which occurs when the lattice distorts to accommodate the excited F center.

The SP models for CaO and CaF_2 predict excessive Stoke's shifts which are not observed for CaO and which are not expected intuitively for CaF_2. The PI(3) model is rather successful for the emission process in CaO. It also explains the absorption process in CaF_2 reasonably well.

Each of the SP models and the PI models has had its successes and failures in explaining the observed properties of the F center in ionic crystals. However, one model which successfully treats all F centers in such classes of crystals as KCl, CaO, and CaF_2 still remains to be constructed.

ACKNOWLEDGMENTS

The author thanks Dr. A. D. Franklin and Professor D. B. Fitchen for helpful discussions. He wishes to thank the personnel of the Aspen Center for Physics for their kind hospitality, where the manuscript was written.

APPENDIX: LIST OF NOTATIONS FOR THE F-CENTER MODELS

A summary of the essential features of each model is given below.

SP(HF, approx): the semicontinuum-polaron model, hydrogenic trial wave functions; continuum Hartree approximation for the optical polarization, Eq. (19); Hamiltonian, Eq. (21), is used for both the absorption and emission states.

SP(HF, exact): the semicontinuum-polaron model; exact numerical solutions; continuum Hartree approximation for the optical polarization, Eq. (19); Hamiltonian, Eq. (21), is used for both the absorption and emission states.

SP(HF_1): the semicontinuum-polaron model; exact numerical solutions; continuum Hartree approximation for the optical polarization, Eq. (19); Hamiltonian, Eqs. (33) and (34), for absorption states; Hamiltonian, Eqs. (35) and (30) for emission states.

SP(QA, approx): same model as the SP(HF, approx.) model except that the quasiadiabatic approximation for the optical polarization, Eq. (18), is used.

SP(QA, exact): same model as the SP(HF, exact)

model except that the quasiadiabatic approximation for the optical polarization, Eq. (18), is used.

SP(QA_1): same model as the SP(HF_1) model except that the quasiadiabatic approximation for the optical polarization, Eq. (18), is used.

SP(EI_1): the semicontinuum-polaron model; exact numerical solutions; the Toyazawa[25] and Haken and Schottky[26] expressions for the electronic polarization, Eq. (37), and the ionic polarization, Eq. (13); Hamiltonian, Eqs. (39) and (40) for absorption states; Hamiltonian, Eqs. (41) and (42), for emission states.

PI(2, approx): the Hartree-Fock polarizable-ion model; hydrodegenic trial wave functions; point-ion potential; evaluation of the polarization potential according to the first-order Mott-Littleton procedure[28]; the polarization potential which arises from the dipoles induced on the first two shells ($n = 1$ and $n = 2$) is treated rigorously and only the spherically symmetric part of the polarization which arises from all the other dipoles on shells $n \geq 3$ is considered; Franck-Condon principle is satisfied for all optical transitions.

PI(3): the polarizable-ion model; exact numerical solutions; point-ion potential; only the ionic polarization of the nearest neighbors is considered; Franck-Condon principle is satisfied for all optical transitions.

---

[1]S. R. Tibbs, Trans. Faraday Soc. 35, 147 (1934).

[2]W. B. Fowler, in *Physics of Color Centers*, edited by W. B. Fowler (Academic, New York, 1968).

[3]J. J. Markham, in *Solid State Physics*, edited by F. Seitz and D. Turnbull (Academic, New York, 1968), Vol. VIII Suppl.

[4]Z. J. Kiss, Phys. Today 23 (No. 1), 42 (1970).

[5]H. Haken, Nuovo Cimento 10, 1230 (1956).

[6]H. Haken, in *Polarons and Excitons*, edited by C. G. Kuper and G. D. Whitfield (Oliver and Boyd, London, 1963), p. 295.

[7]H. S. Bennett, Phys. Rev. 169, 729 (1968).

[8]H. S. Bennett, Phys. Rev. 184, 918 (1969).

[9]The notations SCP and HFPI which occur in Refs. 7 and 8 are changed in this paper to SP and PI, respectively.

[10]R. K. Swank and F. C. Brown, Phys. Rev. 130, 34 (1963).

[11]J. C. Kemp *et al.*, Phys. Rev. 171, 1024 (1968).

[12]B. D. Evans *et al.*, Phys. Letters 27A, 506 (1968).

[13]W. B. Fowler, Phys. Rev. 135, A1725 (1964).

[14]G. Chiarotti *et al.*, Nuovo Cimento 64B, 159 (1969).

[15]Atomic units are used in this paper: 0.529×10^{-8} cm = 1 a.u. of length and 27.2 eV = 1 a. u. of energy.

[16]L. D. Bogan and D. B. Fitchen (unpublished).

[17]H. Kuhnert, Phys. Status Solidi 21, K171 (1967).

[18]L. F. Stiles *et al.*, Phys. Rev. B 2, 2077 (1970).

[19]W. B. Fowler *et al.*, Solid State Commun. 5, 659 (1967).

[20]R. F. Wood and U. Opik, Phys. Rev. 179, 783 (1969).

[21]H. S. Bennett, Bull Am. Phys. Soc. 15, 339 (1970).

[22]The author refers the reader to Ref. 7, p. 738, for a discussion of the additional assumptions needed to treat the oxides.

[23]R. P. Feynman, Phys. Rev. 97, 660 (1955).

[24]G. S. Gourary and F. J. Adrian, in *Solid State Physics*, edited by F. Seitz and D. Turnbull (Academic, New York, 1960), Vol. X, p. 127.

[25]Y. Toyozawa, Progr. Theoret. Phys. (Kyoto) 12, 422 (1954).

[26]H. Haken and W. Schottky, Z. Physik. Chem. (Frankfurt) 16, 218 (1958).

[27]The quantity E_s in V/m is divided by 51.4137×10^{10} to give the energy of the term $eE_s z$ in atomic units.

[28]N. F. Mott and M. J. Littleton, Trans. Faraday Soc. 34, 485 (1938).